

# FIT: Defying Catastrophic Forgetting in Continual LLM Unlearning

Xiaoyu Xu<sup>1</sup> Minxin Du<sup>1</sup> Kun Fang<sup>1</sup> Zi Liang<sup>1</sup> Yixin Xiao<sup>1</sup> Zhicong Huang<sup>2</sup>  
Cheng Hong<sup>2</sup> Qingqing Ye<sup>1</sup> Haibo Hu<sup>1</sup>

## Abstract

Large language models (LLMs) demonstrate impressive capabilities across diverse tasks but raise concerns about privacy, copyright, and harmful materials. Existing LLM unlearning methods rarely consider the continual and high-volume nature of real-world deletion requests, which can cause utility degradation and catastrophic forgetting as requests accumulate. To address this challenge, we introduce FIT, a framework for continual unlearning that handles large numbers of deletion requests while maintaining robustness against both catastrophic forgetting and post-unlearning recovery. FIT mitigates degradation through rigorous data Filtering, Importance-aware updates, and Targeted layer attribution, enabling stable performance across long sequences of unlearning operations and achieving a favorable balance between forgetting effectiveness and utility retention. To support realistic evaluation, we present **PCH**, a benchmark covering **P**ersonal information, **C**opyright, and **H**armful content in sequential deletion scenarios, along with two symmetric metrics, Forget Degree (F.D.) and Retain Utility (R.U.), which jointly assess forgetting quality and utility preservation. Extensive experiments on four open-source LLMs with hundreds of deletion requests show that FIT achieves the strongest trade-off between F.D. and R.U., surpasses existing methods on MMLU, CommonsenseQA, and GSM8K, and remains resistant against both relearning and quantization recovery attacks.<sup>1</sup>

## 1. Introduction

Large language models (LLMs) exhibit remarkable versatility but pose significant ethical and legal risks due to their

<sup>1</sup>The Hong Kong Polytechnic University <sup>2</sup>Ant Group. Correspondence to: Minxin Du <minxin.du@polyu.edu.hk>, Haibo Hu <haibo.hu@polyu.edu.hk>.

Preprint. Under review.

<sup>1</sup>  [https://xiaoyuxu1.github.io/FIT\\_PCH/](https://xiaoyuxu1.github.io/FIT_PCH/)

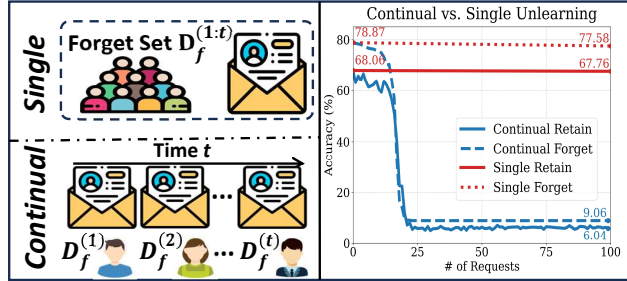


Figure 1. Left: Schematics of *single-shot* vs. *continual* unlearning; Right: Retain and forget accuracy on Yi-6B using GA for single unlearning and 100 sequential request(s), and catastrophic forgetting begins after roughly 25 requests.

tendency to memorize sensitive, harmful, or copyrighted training data (Karamolegkou et al., 2023). To comply with regulations, such as the GDPR (Mantelero, 2013) (“Right to be Forgotten”) and CCPA (Harding et al., 2019), *machine unlearning* has emerged as a critical mechanism for erasing specific data influences without the prohibitive cost of full retraining (Bourtoule et al., 2021; Cao & Yang, 2015).

Unlearning can be exact or approximate (Bourtoule et al., 2021). *Exact unlearning* requires that the distribution of the unlearned model be identical to a model fully retrained on the retain set. SISA (Sharded, Isolated, Sliced, Aggregated) achieves this by training models on partitioned data shards (Bourtoule et al., 2021); when a deletion request arrives, only the affected shard needs retraining. Yet, it is prohibitively expensive for LLMs. So, research has shifted toward the *approximate* case, which relaxes strict distributional guarantees for behavioral similarity. Common methods include gradient ascent (GA), which maximizes loss on the forget set; random label (RLabel), which assigns random targets to forget samples; and negative preference optimization (NPO) (Zhang et al., 2024), which penalizes model preference for forget-set behaviors. While effective at removing targeted information, they often degrade model utility, prompting the development of utility-preserving variants (e.g., GA+GD, NPO+GD) (Yao et al., 2024).

However, they predominantly focus on a *single-shot* setting, where the entire forget set is removed at once. In practice, *continual unlearning* arises, where requests arrive sequen-

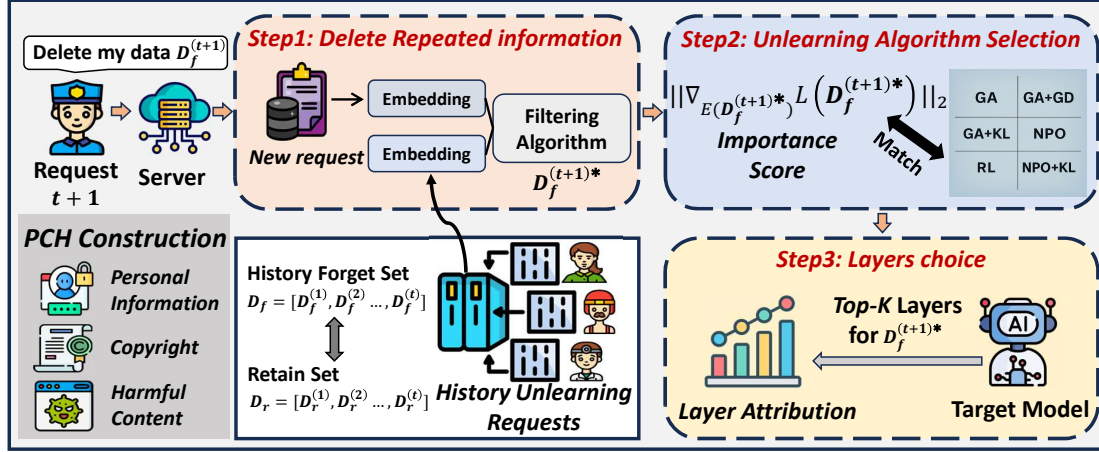


Figure 2. Overview of FIT: Incoming unlearning requests are first de-duplicated via embedding-based redundancy filtering (Section 3.1). For each filtered request, an importance score then guides adaptive selection of the unlearning method (Section 3.2), and targeted layer attribution restricts updates to the top- $K$  influential layers (Section 3.3), mitigating compounded knowledge loss and parameter drift.

tially, repeatedly, and in intertwined forms throughout an LLM’s life cycle (Liu et al., 2025b). Directly extending them by treating each request independently often results in severe utility degradation or even *catastrophic forgetting* (Shi et al., 2025b; Barez et al., 2025; Liu et al., 2025b). As shown in Figure 1, while single-shot removal has minimal impact, continual unlearning causes a rapid decline in both forget and retain accuracy after only a few requests. Similar failure modes have been reported for image models (Thakral et al., 2025; Lee et al., 2025; Zhao et al., 2024a).

Very few recent efforts have addressed specialized continual LLM unlearning. Orthogonal unlearning ( $O^3$ ) (Gao et al., 2025) combines LoRA adapters with an out-of-distribution detector to achieve efficiency. However, detector failures can impede forgetting, and LoRA constraints may increase the risk of reactivating forgotten knowledge (Hu et al., 2025). Other methods, like ALKN (Wuerkaixi et al., 2025), reduce parameter drift via adaptive task vectors but rely on costly gradient inspection. Ultimately, these methods remain vulnerable to catastrophic forgetting under heavy request loads. Furthermore, unlearned models can be vulnerable to post-unlearning recovery triggered by small parameter updates, such as relearning via fine-tuning (Lo et al., 2024; Xu et al., 2025b) and quantization attacks (Zhang et al., 2025).

A natural question arises: *can we achieve the best of both worlds—realizing continual unlearning that retains the versatility of general single-shot methods, while being efficient as tailored designs like  $O^3$ , and ensuring robustness against catastrophic forgetting and post-unlearning recovery?*

## 1.1. Technical Overview

We identify three primary drivers of catastrophic forgetting in continual unlearning: i) cumulative redundancy from se-

mantically similar requests, ii) unstable gradient updates, and iii) excessive parameter drift. Notably, there is an inherent trade-off: large drift leads to failure, whereas insufficient drift leaves the model vulnerable to data recovery.

Guided by these insights, we propose FIT, a framework for continual unlearning in LLMs (Figure 2). The first module mitigates cumulative utility loss caused by repeatedly deleting semantically overlapping requests (Wuerkaixi et al., 2025) by filtering redundant inputs using an embedding-based similarity check and a loss-difference test, ensuring that sensitive information is preserved while redundant content is removed. The second module addresses update instability (Barez et al., 2025) through an importance-aware adaptive mechanism that scores each request and selects an appropriate unlearning algorithm based on its estimated influence, stabilizing gradient directions and avoiding aggressive updates. Our theoretical analysis confirms that these components reduce unstable updates and collapse risk.

The third module curbs parameter drift through a targeted layer-attribution strategy inspired by Shapley-style relevance estimation (Rozemberczki et al., 2022). Instead of updating all layers or relying on fixed rules, it identifies the most influential layers for each request and restricts modifications to these regions. This provides a practical trade-off between recovery robustness and model stability, while simultaneously improving efficiency.

## 1.2. A New Benchmark

Existing unlearning datasets focus almost exclusively on single-shot settings (Maini et al., 2024; Li et al., 2024; Shi et al., 2025b; Jin et al., 2024; Yao et al., 2024) and each targets only one deletion category (Table 1). TOFU (Maini et al., 2024) evaluates fictitious-author removal for privacy,

WMDP (Li et al., 2024) targets hazardous knowledge, and MUSE (Shi et al., 2025b) focuses on copyright deletion using curated news and book text. Reliable evaluation is further hindered by inconsistent metrics: MUSE employs disparate criteria that obscure holistic trade-offs, while TOFU relies on paraphrased answers that introduce bias and uses mismatched evaluation protocols across forget and retain sets, leading to inconsistent results.

To address the lack of a dedicated *continual* unlearning benchmark, we introduce **PCH**, which unifies **P**ersonal information, **C**opyright, and **H**armful content. All instances are synthetically generated by GPT-4o using structured prompts (without real data or violating OpenAI’s usage policies) to reduce overlap with common pre-training corpora, and are manually verified for category consistency and basic distributional properties. These steps enable the construction of faithful retain baselines.

We further propose two symmetric metrics: Forget Degree (F.D.) and Retain Utility (R.U.). Computed as the geometric mean of three underlying measures (on forget and retain sets), they provide a scale-invariant, interpretable assessment that captures the trade-off between forgetting and retention without allowing any single factor to dominate.

Our main contributions are summarized below.

I) We propose **FIT**, a robust continual unlearning framework to defy catastrophic forgetting in LLMs. It integrates three strategic mechanisms: embedding-based redundancy Filtering to prevent gradient accumulation, Importance-aware adaptive algorithm selection to stabilize updates, and Targeted layer attribution to minimize parameter drift.

II) We introduce **PCH**, a unified benchmark explicitly tailored for continual unlearning, spanning **P**ersonal privacy, **C**opyrighted material, and **H**armful content. To address the limitations of existing disparate metrics, we propose two symmetric, aggregate metrics, F.D. and R.U. These metrics provide a scale-invariant and interpretable assessment of the trade-off between forgetting effectiveness and model utility.

III) Experiments across four LLMs and up to 300 sequential unlearning requests show that **FIT** maintains higher utility and stronger forgetting than *all* prior arts, *e.g.*, on Yi-6B, **FIT** achieves roughly +0.20 F.D. and +0.10 R.U. over ALKN and  $O^3$  at 300 requests. While slightly less efficient than  $O^3$  (employing LoRA-based detection), it is more resilient to relearning and quantization attacks.

## 2. Problem Formulation and Preliminaries

### 2.1. Problem Formulation

Let  $D$  denote the entire (pre-)training corpus and  $\mathcal{A}$  the algorithm producing the model  $\mathcal{M} = \mathcal{A}(D)$ . Given a *forget*

set  $D_f \subset D$ , an unlearning operator  $\mathcal{U}$  generates an updated model  $\mathcal{M}_f = \mathcal{U}(\mathcal{M}, D_f)$ . The complement is defined as the *retain set*  $D_r = D \setminus D_f$ . Unlearning generally falls into two categories: *exact* and *approximate* (Bourtoule et al., 2021). Exact unlearning requires the distribution of  $\mathcal{M}_f$  to be identical to that of a model retrained from scratch,  $\mathcal{M}_r = \mathcal{A}(D_r)$ , ensuring all statistical traces of  $D_f$  are removed. However, exact methods (*e.g.*, SISA (Bourtoule et al., 2021)) are prohibitively expensive for modern LLMs. So, we pursue approximate unlearning, which relaxes strict equivalence in favor of behavioral or distributional similarity (Yao et al., 2024; Maini et al., 2024; Shi et al., 2025b).

While most existing work focuses on *single-shot* unlearning (Yao et al., 2024; Pawelczyk et al., 2024; Li et al., 2024; Wang et al., 2025; Song et al., 2025), where  $\mathcal{U}$  is invoked once for a single forget set  $D_f$ . Instead, we address the more realistic—yet scarcely explored—*continual unlearning* scenario. Here, unlearning requests  $D_f^{(1)}, \dots, D_f^{(t)}$  arrive sequentially, reflecting real-world online deletion demands. At round  $t$ , the cumulative forget set is  $D_f^{(1:t)} = \bigcup_{i=1}^t D_f^{(i)}$ , with the corresponding retain set  $D_r^{(1:t)} = D \setminus D_f^{(1:t)}$ . The model updates iteratively:  $\mathcal{M}_f^{(i)} = \mathcal{U}(\mathcal{M}_f^{(i-1)}, D_f^{(i)})$ . Naïve sequential application of  $\mathcal{U}$  often degrades utility rapidly, leading to catastrophic forgetting (Shi et al., 2025b).

Our threat model (Appendix G) considers this instability alongside adversarial risks, including “*malicious*” *unlearning* with a large volume of requests (*cf.* denial of service) to induce collapse (Barez et al., 2025), *relearning attacks* (Lo et al., 2024), and *quantization attacks* (Zhang et al., 2025).

**Practical evaluation.** Ideally, the unlearning quality at round  $i$  is measured against a “gold-standard” retrained model  $\mathcal{M}_r^{(i)} = \mathcal{A}(D_r^{(1:i)})$ . Since full retraining on the unavailable corpus  $D$  is infeasible, we adopt the synthetic proxy approach from (Maini et al., 2024). We synthesize disjoint datasets “ $D_f$ ” and “ $D_r$ .” We then: i) fine-tune  $\mathcal{M}$  on the union  $D_f \cup D_r$  to embed the knowledge, and ii) fine-tune a separate copy of  $\mathcal{M}$  solely on  $D_r$  to serve as the *retain model*. This surrogate provides a rigorous baseline for evaluating both deletion fidelity and utility preservation.

### 2.2. Common (Single-shot) Unlearning Methods

We use three classes of single-shot methods as primitives. **(i) GA Family:** It maximizes loss on  $D_f$  while preserving performance on  $D_r$ :  $\mathcal{L} = \mathcal{L}_{\text{GA}}(D_f) + \lambda \mathcal{L}_{\text{retain}}(D_r)$ , where  $\lambda \geq 0$ . Variants include pure GA ( $\lambda = 0$ ), GA+GD (with cross-entropy on  $D_r$ ), and GA+KL (with KL divergence to a reference model) (Yao et al., 2024).

**(ii) NPO Family:** It prevents over-forgetting by penalizing the model’s alignment with  $D_f$  rather than maximizing loss (Zhang et al., 2024):  $\mathcal{L} = \mathcal{L}_{\text{NPO}}(D_f) + \lambda \mathcal{L}_{\text{retain}}(D_r)$ .

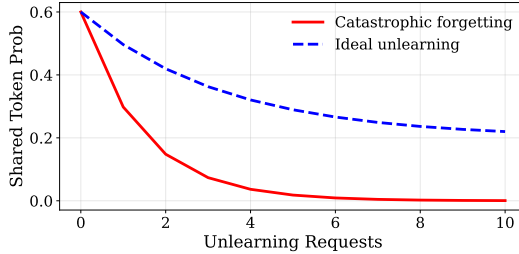


Figure 3. Estimated decay of shared-token probabilities as semantically similar requests are iteratively removed: Redundant gradients push them toward near zero, causing model collapse, whereas effective unlearning stabilizes them at moderate, non-zero levels.

The NPO+KL variant applies KL divergence on  $D_r$ .

(iii) **RLabel**: It enforces uniform predictions by training on random labels for  $D_f$  (Yao et al., 2024):  $\mathcal{L} = \mathcal{L}_{\text{RLabel}}(D_f)$ .

Each method presents a trade-off: aggressive strategies like GA ensure forgetting but risk severe utility degradation (or over-forgetting) (Yao et al., 2024). Conversely, NPO and regularized variants better preserve utility but may be less effective at erasing knowledge (Zhang et al., 2024).

### 3. Our Approach: FIT

Continual unlearning in LLMs requires maintaining utility as unlearning requests accumulate. Our analysis identifies three primary drivers of collapse: i) the cumulative removal of semantically similar content, ii) unstable gradient updates across sequential steps, and iii) excessive parameter drift from indiscriminate updates (Wuerkaixi et al., 2025).

To address these challenges, we propose **FIT**, a continual unlearning framework designed to handle high-volume unlearning requests while ensuring robustness against catastrophic forgetting and post-unlearning recovery. It comprises three primary modules (Figure 2): i) an embedding-based Filtering module that prunes redundant requests to prevent compounded knowledge loss, ii) an Importance-aware adaptive algorithm that stabilizes updates via gradient-based data attribution (Ancona et al., 2018), and iii) a Targeted layer-attribution mechanism, inspired by Shapley values (Rozemberczki et al., 2022), that restricts updates to highly influential layers to curb parameter drift.

#### 3.1. Redundancy Filtering

Unlearning requests (from diverse sources) often contain semantically similar text, such as recurrent descriptions of a theoretical concept or repeated references to a specific entity. When such requests are sequentially removed, their overlapping gradients accumulate along shared lexical dimensions, driving a systematic suppression of common tokens rather than targeted removal of specific memories (Wuerkaixi et al.,

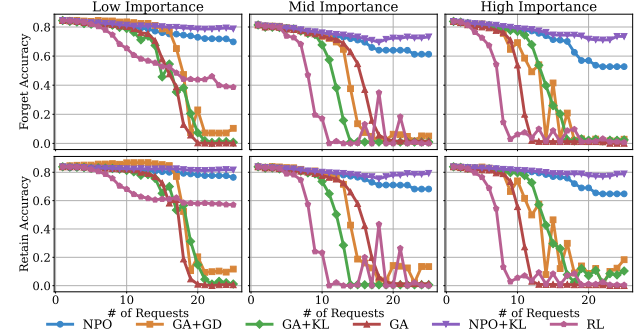


Figure 4. Performance of the unlearning methods across importance levels: Rows trace the forgetting and retain accuracy curves; columns represent the low, medium, and high. Our goal is to select unlearning algorithms for low forget and high retain accuracy.

2025). Figure 3 illustrates an estimated decay curve derived from the redundancy analysis in Appendix A.1; it predicts that repeated updates precipitate a collapse of shared-token probabilities toward zero. Once these tokens collapse, the model loses the semantic distinctions they support, resulting in catastrophic forgetting. Ideally, unlearning mechanisms should prevent this collapse by stabilizing token probabilities at moderate, non-zero levels, thereby reducing reliance on targeted information while preserving the semantic capacity necessary for coherent generation.

A conventional approach to mitigating redundancy involves filtering incoming requests based on their similarity to historical data via embedding-based metrics. However, semantic similarity does not strictly equate to redundancy; texts may exhibit substantial lexical overlap while conveying distinct personal attributes or harmful contexts. Such filtering must navigate two competing risks: aggressive filtering may discard legitimately forgettable content, leading to information leakage, whereas insufficient filtering exacerbates gradient overlap, increasing the risk of catastrophic forgetting.

To balance redundancy reduction with knowledge preservation, we propose a two-stage filtering protocol. Given a history  $D_f^{(1:t)}$  and a new request  $D_f^{(t+1)}$ , we generate a filtered request  $D_f^{(t+1)*}$  and update the history to  $D_f^{(1:t+1)}$ . In the first stage, we partition  $D_f^{(t+1)}$  into fixed-size chunks. For each chunk  $x$ , we compute its embedding  $e(x)$  using SimCSE (Gao et al., 2021) and identify the maximum cosine similarity  $s^*$  against the history set. If  $s^*$  falls below a threshold  $\tau$ , the chunk is marked as a candidate for removal.

However, high similarity scores can be misleading; distinct sentences may share lexical structure (e.g., “My name is Alice” vs. “My name is Bob”) while containing specific tokens, such as PII, that carry unique semantic roles. To prevent the loss of such informative content, we introduce a

Table 1. Overview of existing benchmarks, where ‘‘GPT & Human’’ indicates datasets constructed from GPT-generated candidates that are subsequently verified or refined by human annotators.

Dataset	Data Types	Retain Model	Method
MUSE (Shi et al., 2025b)	Copyright	✓	GPT&Human
TOFU (Maini et al., 2024)	Personal information	✓	GPT&Human
WMDP (Li et al., 2024)	Harmful content	✗	Human
WPU (Liu et al., 2024b)	Copyright	✗	GPT&Human
RWKU (Jin et al., 2024)	Personal information	✗	GPT&Human

secondary *loss-difference test*. We compute:

$$\Delta L = |L_{\text{with}} - L_{\text{without}}|, \quad (1)$$

where  $L_{\text{with}}$  and  $L_{\text{without}}$  denote the cross-entropy loss computed on  $\mathcal{D}_f^{(t+1)}$  and  $\mathcal{D}_f^{(t+1)} \setminus x$ , respectively. A significant  $\Delta L$  suggests that  $x$  contributes non-trivial information to the model’s predictions, aligned with our analysis in Appendix A.1. Consequently, if  $\Delta L > \epsilon$ , the chunk is retained regardless of its similarity score; otherwise, discarded. The pseudocode is detailed in Algorithm 1 (Appendix A.1).

We utilize GPT-4o sensitivity scoring as a consistency check for sensitive token retention (Gu et al., 2024), while term-distribution visualizations quantify the preservation strength of these tokens. Appendix A.1 demonstrates that our two-stage approach effectively removes redundant content while preserving semantically sensitive tokens, including names, harmful terms, and copyright-relevant expressions.

### 3.2. Importance-Guided Algorithm Selection

Applying the same unlearning algorithm to a model that has already undergone previous requests results in repeatedly-aligned update directions, hence gradient instability and accumulated parameter shift (see Appendix A.2). Dynamically switching between unlearning methods allows the update strength and gradient direction to adapt to the specific characteristics of each request, yielding more stable parameter updates. Since our framework utilizes a pool of single-shot unlearning methods, the critical challenge lies in selecting the optimal one for each filtered request.

Deletion efficacy is known to correlate with sample memorization (Zhao et al., 2024b): highly memorized samples require stronger unlearning objectives, whereas weaker ones do not. This indicates that method selection should adapt to the memorization level of incoming requests. However, computing memorization scores for each request is computationally infeasible, as classical estimators require expensive forward-backward procedures. This motivates the need for a lightweight proxy that can guide method choice efficiently.

To address this, we introduce a lightweight importance score,  $\text{IMP}$ , and select the unlearning algorithm accordingly. Inspired by gradient-based attribution (Ancona et al., 2018),  $\text{IMP}$  measures the sensitivity of the loss with respect to

a request’s embedding, serving as a proxy for its training influence. This approach enables request-level adaptation without the overhead of memorization-based metrics. For a new filtered request  $\mathcal{D}_f^{(t+1)*}$ , we compute the  $\ell_2$  norm of the gradient with respect to its embedding:

$$\text{IMP}\left(L(\mathcal{D}_f^{(t+1)*})\right) = \left\| \nabla_{E(\mathcal{D}_f^{(t+1)*})} L(\mathcal{D}_f^{(t+1)*}) \right\|_2, \quad (2)$$

where  $E(\cdot)$  denotes the embedding function. The input-gradient norm measures loss sensitivity to the request influence; while not a direct memorization metric, it often correlates with how strongly the model relies on the request.

Following (Zhao et al., 2024b), we discretize  $\text{IMP}$  scores into three levels (low, medium, high) to select from six standard unlearning methods (see Section 2.2). Our analysis (Appendix A.2) and empirical results (Figure 4) indicate that unlearning efficacy depends on aligning update strength with the request’s  $\text{IMP}$ . Low- $\text{IMP}$  ones are best handled by aggressive methods (e.g., RLabel) to achieve strong forgetting with minimal utility cost. Medium- $\text{IMP}$  ones benefit from moderated methods like NPO that balance forgetting and retention. High- $\text{IMP}$  ones require conservative methods (e.g., NPO+KL) to preserve utility while tolerating slight residual memorization. Thus, adapting unlearning strength to  $\text{IMP}$  outperforms fixed policies by explicitly coupling update magnitude with request influence.

### 3.3. Targeted Layer Attribution

Continual unlearning faces a fundamental trade-off: updating all layers incurs high computational costs and degrades utility, whereas sparse updates improves efficiency but increases vulnerability to post-unlearning recovery.

Existing selective update strategies have limitations. Freezing bottom layers (Zheng et al., 2025) or updating the last  $K$  layers (Goel et al., 2022) ignores the fact that memorized information is distributed differently across layers for different requests. These static, narrowly scoped updates fail to track the shifting directions inherent in continual unlearning. Similarly, LoRA-based methods, such as  $O^3$  (Gao et al., 2025), restrict updates to low-rank adapters while leaving backbone weights unchanged; this allows parameters encoding the forget set to persist, rendering the model susceptible to knowledge reactivation (Hu et al., 2025).

Furthermore, model-editing methods like AlphaEdit (Fang et al., 2025) (constraining updates to null-space directions) and PISCES (Gur-Arieh et al., 2025) (using feature-level masking) also restrict updates to narrow parameter subsets (see Appendix A.3). They rely on localization mechanisms that assume edit-relevant parameters are fixed and spatially localized. While suitable for inserting specific facts, this assumption does not hold for unlearning, where the knowledge to be removed is typically distributed across layers.

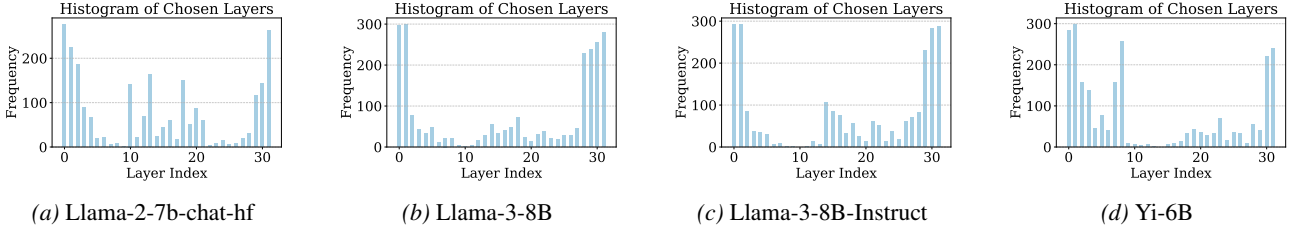


Figure 5. Histogram of layer selection: Each bar shows the frequency with which the corresponding layer was chosen.

Indeed, PISCES demonstrates that AlphaEdit remains vulnerable to recovery. While PISCES improves robustness, it still exhibits recoverability under relearning attacks.

These underscore that effective unlearning requires modifying a broader, dynamically shifting set of parameters. We address this via a request-dependent layer attribution analysis to identify a top- $K$  relevant layers. With an appropriately chosen  $K$ , updates focus on the layers where forget-related representations actually reside, avoiding unnecessary modifications to unrelated components. This enhances stability and efficiency while maintaining compatibility with transferable localization signals from model-editing methods.

**Layer Selection.** We denote the  $K$  most influential layers by  $\mathcal{S}_{\text{top-}K}$ . To identify them, we estimate the contribution of layer  $\ell$  by masking it and measuring the loss deviation:

$$s_\ell = \left| L_{\text{mask}}^{(\ell)} - L_{\text{orig}} \right|,$$

where  $L_{\text{orig}}$  is the original loss and  $L_{\text{mask}}^{(\ell)}$  is the loss after zeroing layer  $\ell$ . This metric approximates Shapley values (Rozemberczki et al., 2022), capturing the marginal effect of a layer on the specific unlearning request. We rank layers by  $s_\ell$  and update only the MLP blocks and attention modules (as they dominate a layer’s functional expressivity) of the top  $K$ , keeping all other parameters frozen. It ensures that updates are focused on components with the highest functional relevance (see Appendix A.3).

**Choosing  $K$ .** To determine the optimal  $K$ , we analyzed layer-selection patterns across four models (Llama-2-7B-chat-hf, Llama-3-8B, Llama-3-8B-Instruct, and Yi-6B). Figure 5 illustrates the frequency with which each layer was selected. Across all models, a compact subset of 6–9 layers is consistently identified as important, suggesting that unlearning is driven by specific regions rather than the entire network. Ablation studies varying the number of updated layers confirm that  $K = 8$  offers the optimal trade-off between robustness and utility. Our targeted approach prevents over-updating while mitigating the recovery vulnerabilities inherent in static or highly restricted update strategies.

## 4. PCH: A Unified Benchmark

### 4.1. The PCH Dataset

*Limitations of current datasets.* Existing unlearning corpora primarily target single-request settings, leaving continual unlearning unexplored (Yuan et al., 2025). TOFU is synthetic (GPT-4 generated with human filtering to enhance diversity and reduce pretraining leakage) and provides a reference retain model for controlled evaluation (Maini et al., 2024). MUSE targets copyright-related deletion with realistic large-scale news and book text, offering structured forget/retain/holdout splits; GPT-4 generates question–answer pairs for each excerpt (Shi et al., 2025b). WMDP focuses on hazardous knowledge removal, with examples manually constructed by experts (Li et al., 2024). As summarized in Table 1, each dataset centers on a single deletion type: TOFU and RWKU on personal information, MUSE and WPU on copyright violations, and WMDP on harmful content, yielding a narrow view of unlearning scenarios. Moreover, real-world requests often involve multiple information types, and directly unifying existing datasets is challenging due to the heterogeneous construction pipelines.

We introduce **PCH**, a unified dataset spanning **P**ersonal information, **C**opyright, and **H**armful content, explicitly tailored for continual unlearning (see Appendix E.1 Figure 13). All samples are generated by GPT-4o and verified by human for category consistency and basic distributional properties (e.g., text length and token-frequency). Here, “harmful content” means semantically harmful text (e.g., rumors) rather than genuinely unsafe material (OpenAI, 2024).

Each category contains 200 samples. The entire set of 600 instances is randomly split into forget and retain subsets. Prompts enforce the constraint “avoid using pre-trained datasets” to reduce overlap with common pretraining corpora, ensuring retain examples are unseen by the base model. As shown in Figure 11 (Appendix E.1), a model fine-tuned on the retain set begins with low accuracy but improves steadily, confirming that **PCH** is out-of-distribution. To evaluate forgetting and utility, each instance is converted into a question–answer (QA) pair (Appendix E.2, Table 6).

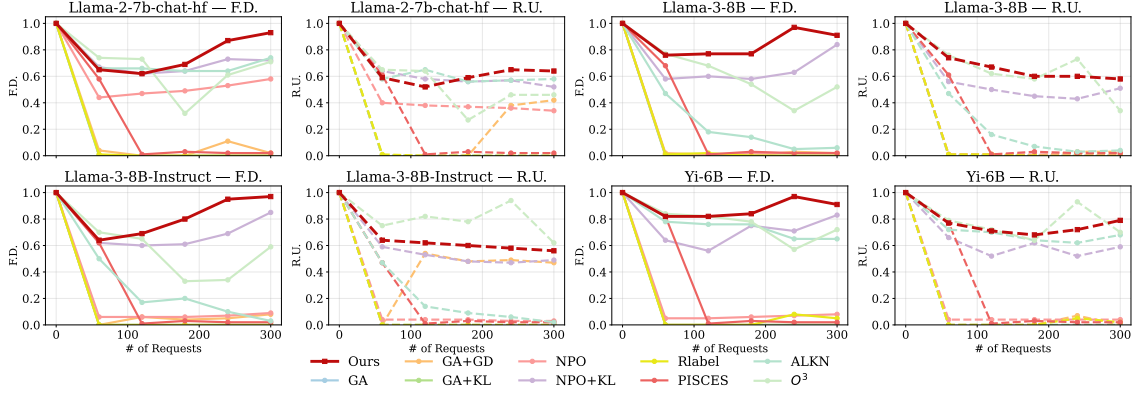


Figure 6. Forget Degree (F.D.) and Retain Utility (R.U.) for each model with increasing number of unlearning requests

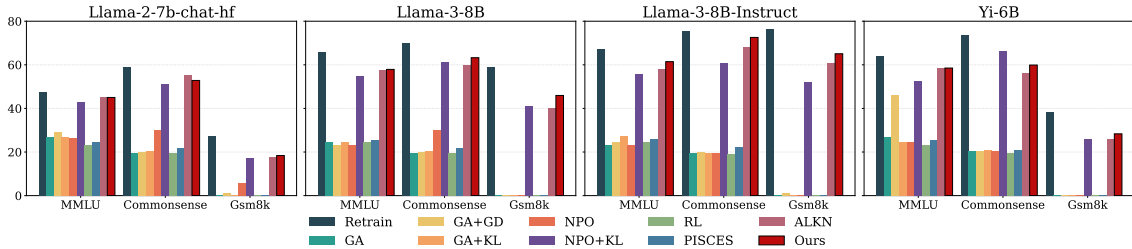


Figure 7. Downstream accuracy on MMLU, CommonsenseQA, and Gsm8k for all models and unlearning methods

## 4.2. Symmetric Metrics for Forgetting and Utility

*Limitations of current metrics.* Only TOFU and MUSE release a retain model, enabling direct comparison between an unlearned model and its original counterpart. MUSE reports four distinct metrics: verbatim memorization, knowledge memorization, privacy leakage, and utility preservation, without a single aggregate score. This heterogeneity can overweight individual metrics and obscure overall performance, underscoring the need for an integrated measure. TOFU combines Forget Quality and Model Utility but i) relies on paraphrase-based answers introducing bias, and ii) applies different evaluation protocols to the forget and retain splits, yielding inconsistent results (Maini et al., 2024).

For remedy, **PCH** is deliberately constructed to be out-of-distribution with respect to pre-training data, so that a model fine-tuned on  $D_r$  alone serves as the retain model, while a model fine-tuned on  $D_f \cup D_r$  serves as the fine-tuned model. We avoid TOFU’s costly paraphrasing and adopt three lightweight, base metrics: Probability, ROUGE-L, and token-level Accuracy; see Appendix D. Each metric is applied *identically* to the forget and retain sets, enabling consistent measurement of both forgetting and utility.

**Our aggregated metrics.** Unlearning evaluation benefits from a single statistic that captures forget-retain trade-offs without being dominated by any one component. Follow-

ing a similar philosophy to TOFU’s normalized aggregation (Maini et al., 2024), we derive two symmetric quantities from the three base metrics. For the forget and retain sets, we compute the *geometric mean*:

$$F = (\text{Prob}_{\text{Forget}} \cdot \text{ROUGE}_{\text{Forget}} \cdot \text{Acc}_{\text{Forget}})^{1/3}, \quad (3)$$

$$R = (\text{Prob}_{\text{Retain}} \cdot \text{ROUGE}_{\text{Retain}} \cdot \text{Acc}_{\text{Retain}})^{1/3}, \quad (4)$$

and similarly obtain  $FQ$  and  $RQ$  for retain model. The geometric mean balances improvements and prevents any single metric from dominating the aggregate.

Based on them, we further define two regularized measures:

$$\text{F.D.} = \max(0, 1 - |F/FQ - 1|), \quad (5)$$

$$\text{R.U.} = \max(0, 1 - |R/RQ - 1|). \quad (6)$$

Forget Degree (F.D.) and Retain Utility (R.U.) measure alignment to the retain model on the forget and retain sets, respectively; since the retain model approximates a retrained model, our goal is closer alignment to the retain model, rather than “larger  $R$  / smaller  $F$  is always better.”

Figure 12 (Appendix D) illustrates these properties. Panels (a–c) plot the geometric mean of two metrics while fixing the third at 0.7; the sharp decline from a single weak component shows that the geometric mean strongly penalizes imbalance, confirming its suitability as a balanced aggregator. Panel (d)

shows F.D. as a function of  $F/FQ$ , exhibiting a symmetric, approximately linear drop from the optimum. It also means that F.D. is scale-invariant and interpretable.

## 5. Experiment

### 5.1. Experimental Setup

**Dataset.** All experiments are run on our **PCH** benchmark.

**Models.** We evaluate FIT on four widely used open-source LLMs : Yi-6B (Young et al., 2024), Llama-2-7b-chat-hf (Touvron et al., 2023), Llama-3-8B (Dubey et al., 2024), and Llama-3-8B-Instruct (Dubey et al., 2024). Since the pre-training corpus  $D$  is unavailable, retraining on  $D_r$  is infeasible. As outlined in Section 2.1 and Appendix B.1, we instead construct synthesis “ $D_f$ ” and “ $D_r$ ,” from which we derive a *fine-tuned model* and a *retain model* as proxies.

**Baselines.** We evaluate our framework against several representative unlearning algorithms: GA, GA+GD, GA+KL, NPO, NPO+KL, RLabel, PISCES (Gur-Arieh et al., 2025),  $O^3$  (Gao et al., 2025), and ALKN (Wuerkaixi et al., 2025).

**Evaluation Metrics.** We use the two proposed metrics, F.D. and R.U., to quantify the forgetting effectiveness and utility preservation. Downstream performance is reported on MMLU (Hendrycks et al., 2021), CommonsenseQA (Talmor et al., 2019), and Gsm8K (Cobbe et al., 2021). Implementation details are provided in Appendix B.

Post-unlearning recovery is evaluated under two settings: i) *Relearning via fine-tuning* (Xu et al., 2025b): an unlearned model is finetuned on *retain* and/or *unrelated* data. Assuming attacker access to forget set is unrealistic and negates the privacy goal; ii) *Quantization attacks* (Zhang et al., 2025): model weights are compressed to `int4`, which can realign residual parameters and revive forgotten information.

### 5.2. Forgetting-Utility Trade-off

Figure 6 summarizes the overall trends in F.D. and R.U. across all models as the number of unlearning requests increases, and Figure 8 provides detailed curves for Llama-3-8B. Across settings, FIT consistently attains the most favorable balance between forgetting and utility. Utility-oriented methods such as NPO+KL,  $O^3$ , and ALKN occasionally obtain higher R.U. (e.g.,  $O^3$  on Llama-3-8B-Instruct), yet this often comes with a noticeable reduction in F.D., indicating insufficient forgetting. These observations highlight the difficulty of maintaining utility without compromising deletion fidelity under sequential unlearning.

Figure 7 reports accuracy on MMLU, CommonsenseQA, and Gsm8K. FIT preserves generalization and avoids the utility collapse observed in aggressive baselines (RLabel, GA, PISCES). While ALKN and NPO+KL approach our

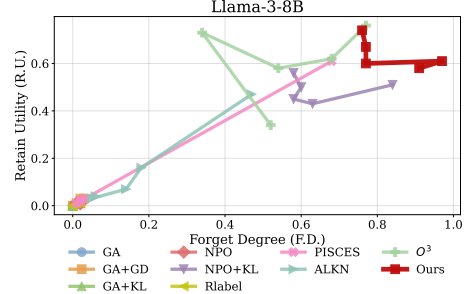


Figure 8. Performance of different methods on Llama-3-8B. Each curve connects 60/120/180/240/300 unlearning requests; points nearer the upper-right corner indicate a better trade-off.

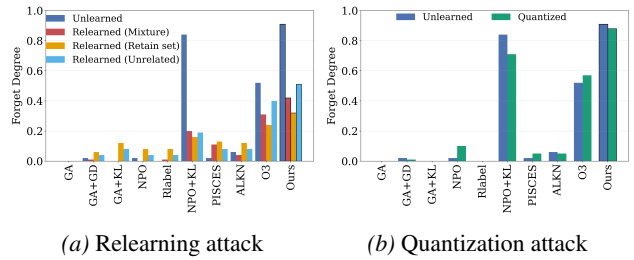


Figure 9. Robustness comparison of unlearning methods on Llama-3-8B under relearning and quantization attacks

performance on simpler tasks, they are less stable on challenging datasets like Gsm8K. We exclude  $O^3$  from these evaluations due to incompatibility with the benchmark infrastructure (Contributors, 2023), which enforces fixed input-output protocols that conflict with  $O^3$ ’s dynamic OOD-based detection, hindering reproducibility and fairness.

We also conduct ablation studies to assess the contribution of each component and compare efficiency (e.g., memory consumption) against baselines, as detailed in Appendix F.

### 5.3. Post-unlearning Recovery

**Relearning via fine-tuning.** Figure 9(a) shows results when further fine-tuning unlearned models on: i) mixed retain and unrelated data, ii) retain-only, and iii) unrelated-only. All methods exhibit reduced F.D., indicating partial recovery, while our approach remains the most robust across settings.

**Quantization.** Compressing models to `int4` amplifies residual memorization and can revive information; see Figure 9(b) Most baselines experience a pronounced drop in F.D., whereas ours maintains high F.D. under quantization.

## 6. Conclusion

We introduced FIT, a scalable framework for continual unlearning in LLMs that supports high-volume unlearning requests while maintaining robustness against catastrophic for-

getting and post-unlearning recovery. FIT mitigates degradation through rigorous data Filtering, Importance-aware updates, and Targeted layer attribution. To enable realistic evaluation, we proposed the **PCH** benchmark, which unifies **P**ersonal information, **C**opyright, and **H**armful content, together with two symmetric metrics—Forget Degree (F.D.) and Retain Utility (R.U.)—for reliable measurement. Experiments show that FIT improves both *F.D.* and *R.U.*, achieves higher accuracy on downstream tasks such as GSM8K and MMLU under continual unlearning, and remains resilient to quantization-based and relearning-based recovery attacks.

## Impact Statement

Our work studies continual unlearning in large language models to improve privacy and security. The **PCH** benchmark is fully synthetic, generated with GPT-4o, and ensures that no real personal data, copyrighted material, or harmful content is included. All samples are fictitious and controlled, minimizing risks to individuals, organizations, and the public. We also incorporate FIT to guide where and how updates are applied during unlearning, aiming to reduce unintended side effects under sequential requests. Our analysis of recovery attempts (*e.g.*, relearning via fine-tuning or quantization attacks) is conducted only to evaluate robustness and inform safer designs, not to enable misuse. We believe the benefits of stronger and more reliable unlearning outweigh the limited risks, and we take appropriate precautions throughout data construction and experimentation.

## References

Ancona, M., Ceolini, E., Öztireli, C., and Gross, M. Towards better understanding of gradient-based attribution methods for deep neural networks. In *ICLR*, 2018.

Barez, F., Fu, T., Prabhu, A., Casper, S., Sanyal, A., Bibi, A., O’Gara, A., Kirk, R., Bucknall, B., Fist, T., Ong, L., Torr, P., Lam, K., Trager, R., Krueger, D., Minderharm, S., Hernández-Orallo, J., Geva, M., and Gal, Y. Open problems in machine unlearning for AI safety. arXiv:2501.04952, 2025.

Bouroule, L., Chandrasekaran, V., Choquette-Choo, C. A., Jia, H., Travers, A., Zhang, B., Lie, D., and Papernot, N. Machine unlearning. In *S&P*, pp. 141–159, 2021.

Cao, Y. and Yang, J. Towards making systems forget with machine unlearning. In *S&P*, pp. 463–480, 2015.

Carlini, N., Tramèr, F., Wallace, E., Jagielski, M., Herbert-Voss, A., Lee, K., Roberts, A., Brown, T. B., Song, D., Erlingsson, Ú., Oprea, A., and Raffel, C. Extracting training data from large language models. In *USENIX Security*, pp. 2633–2650, 2021.

Cobbe, K., Kosaraju, V., Bavarian, M., Chen, M., Jun, H., Kaiser, L., Plappert, M., Tworek, J., Hilton, J., Nakano, R., Hesse, C., and Schulman, J. Training verifiers to solve math word problems. arXiv:2110.14168, 2021.

Contributors, O. Opencompass: A universal evaluation platform for foundation models. <https://github.com/open-compass/opencompass>, 2023.

Dubey, A., Jauhri, A., Pandey, A., Kadian, A., Al-Dahle, A., Letman, A., Mathur, A., Schelten, A., Yang, A., Fan, A., Goyal, A., Hartshorn, A., Yang, A., Mitra, A., Sravankumar, A., Korenev, A., Hinsvark, A., Rao, A., Zhang, A., Rodriguez, A., Gregerson, A., Spataru, A., Rozière, B., Biron, B., Tang, B., Chern, B., Caucheteux, C., Nayak, C., Bi, C., Marra, C., McConnell, C., Keller, C., Touret, C., Wu, C., Wong, C., Ferrer, C. C., Nikolaidis, C., Al-lonsius, D., Song, D., Pintz, D., Livshits, D., Esiobu, D., Choudhary, D., Mahajan, D., Garcia-Olano, D., Perino, D., Hupkes, D., Lakomkin, E., AlBadawy, E., Lobanova, E., Dinan, E., Smith, E. M., Radenovic, F., Zhang, F., Synnaeve, G., Lee, G., Anderson, G. L., Nail, G., Mialon, G., Pang, G., Cucurell, G., Nguyen, H., Korevaar, H., Xu, H., Touvron, H., Zarov, I., Ibarra, I. A., Kloumann, I. M., Misra, I., Evtimov, I., Copet, J., Lee, J., Geffert, J., Vranes, J., Park, J., Mahadeokar, J., Shah, J., van der Linde, J., Billock, J., Hong, J., Lee, J., Fu, J., Chi, J., Huang, J., Liu, J., Wang, J., Yu, J., Bitton, J., Spisak, J., Park, J., Rocca, J., Johnstun, J., Saxe, J., Jia, J., Alwala, K. V., Upasani, K., Plawiak, K., Li, K., Heafield, K., Stone, K., and et al. The llama 3 herd of models. arXiv:2407.21783, 2024.

Fang, J., Jiang, H., Wang, K., Ma, Y., Shi, J., Wang, X., He, X., and Chua, T. Alphaedit: Null-space constrained knowledge editing for language models. In *ICLR*, 2025.

Gao, C., Wang, L., Ding, K., Weng, C., Wang, X., and Zhu, Q. On large language model continual unlearning. In *ICLR*, 2025.

Gao, T., Yao, X., and Chen, D. Simcse: Simple contrastive learning of sentence embeddings. In *EMNLP*, pp. 6894–6910, 2021.

Geva, M., Bastings, J., Filippova, K., and Globerson, A. Dissecting recall of factual associations in auto-regressive language models. In *EMNLP*, pp. 12216–12235, 2023.

Goel, S., Prabhu, A., Sanyal, A., Lim, S.-N., Torr, P., and Kumaraguru, P. Towards adversarial evaluations for inexact machine unlearning. arXiv:2201.06640, 2022.

Gu, J., Jiang, X., Shi, Z., Tan, H., Zhai, X., Xu, C., Li, W., Shen, Y., Ma, S., Liu, H., Wang, Y., and Guo, J. A survey on llm-as-a-judge. arXiv:2411.15594, 2024.

Gur-Arieh, Y., Suslik, C. H., Hong, Y., Barez, F., and Geva, M. Precise in-parameter concept erasure in large language models. In *EMNLP*, pp. 18997–19017, 2025.

Harding, E. L., Vanto, J. J., Clark, R., Hannah Ji, L., and Ainsworth, S. C. Understanding the scope and impact of the California consumer privacy act of 2018. *Journal of Data Protection & Privacy*, 2(3):234–253, 2019.

Hendrycks, D., Burns, C., Basart, S., Zou, A., Mazeika, M., Song, D., and Steinhardt, J. Measuring massive multitask language understanding. In *ICLR*, 2021.

Hu, E. J., Shen, Y., Wallis, P., Allen-Zhu, Z., Li, Y., Wang, S., Wang, L., and Chen, W. Lora: Low-rank adaptation of large language models. In *ICLR*, 2022.

Hu, H., Wang, S., Dong, T., and Xue, M. Learn what you want to unlearn: Unlearning inversion attacks against machine unlearning. In *S&P*, pp. 3257–3275, 2024.

Hu, S., Fu, Y., Wu, S. Z., and Smith, V. Unlearning or obfuscating? jogging the memory of unlearned llms via benign relearning. In *ICLR*, 2025.

Ilharco, G., Ribeiro, M. T., Wortsman, M., Schmidt, L., Hajishirzi, H., and Farhadi, A. Editing models with task arithmetic. In *ICLR*, 2023.

Jang, J., Yoon, D., Yang, S., Cha, S., Lee, M., Logeswaran, L., and Seo, M. Knowledge unlearning for mitigating privacy risks in language models. In *ACL*, pp. 14389–14408, 2023.

Jin, Z., Cao, P., Wang, C., He, Z., Yuan, H., Li, J., Chen, Y., Liu, K., and Zhao, J. RWKU: benchmarking real-world knowledge unlearning for large language models. In *NeurIPS*, 2024.

Karamolegkou, A., Li, J., Zhou, L., and Søgaard, A. Copyright violations and large language models. In *EMNLP*, pp. 7403–7412, 2023.

Lee, J., Mai, Z., Fan, C., and Chao, W.-L. An empirical exploration of continual unlearning for image generation. In *ICML 2025 Workshop on Machine Unlearning for Generative AI*, 2025.

Lewis, P., Perez, E., Piktus, A., Petroni, F., Karpukhin, V., Goyal, N., Küttler, H., Lewis, M., Yih, W., Rocktaschel, T., Riedel, S., and Kiela, D. Retrieval-augmented generation for knowledge-intensive NLP tasks. In *NeurIPS*, 2020.

Li, N., Pan, A., Gopal, A., Yue, S., Berrios, D., Gatti, A., Li, J. D., Dombrowski, A., Goel, S., Mukobi, G., Helm-Burger, N., Lababidi, R., Justen, L., Liu, A. B., Chen, M., Barrass, I., Zhang, O., Zhu, X., Tamirisa, R., Bharathi, B., Herbert-Voss, A., Breuer, C. B., Zou, A., Mazeika, M., Wang, Z., Oswal, P., Lin, W., Hunt, A. A., Tienken-Harder, J., Shih, K. Y., Talley, K., Guan, J., Steneker, I., Campbell, D., Jokubaitis, B., Basart, S., Fitz, S., Kumaraguru, P., Karmakar, K. K., Tupakula, U. K., Varadarajan, V., Shoshitaishvili, Y., Ba, J., Esveld, K. M., Wang, A., and Hendrycks, D. The WMDP benchmark: Measuring and reducing malicious use with unlearning. In *ICML*, 2024.

Li, Z., Wang, X., Shen, W. F., Kurmanji, M., Qiu, X., Cai, D., Wu, C., and Lane, N. D. Editing as unlearning: Are knowledge editing methods strong baselines for large language model unlearning? arXiv:2505.19855, 2025.

Liu, C. Y., Wang, Y., Flanigan, J., and Liu, Y. Large language model unlearning via embedding-corrupted prompts. In *NeurIPS*, 2024a.

Liu, R., Feng, W., Zhang, T., Zhou, W., Cheng, X., and Ng, S. Rethinking machine unlearning in image generation models. In *CCS*, 2025a.

Liu, S., Yao, Y., Jia, J., Casper, S., Baracaldo, N., Hase, P., Yao, Y., Liu, C. Y., Xu, X., Li, H., et al. Rethinking machine unlearning for large language models. *Nature Machine Intelligence*, pp. 1–14, 2025b.

Liu, Y., Zhang, Y., Jaakkola, T. S., and Chang, S. Revisiting who’s harry potter: Towards targeted unlearning from a causal intervention perspective. In *EMNLP*, pp. 8708–8731, 2024b.

Lo, M., Barez, F., and Cohen, S. B. Large language models relearn removed concepts. In *Findings of ACL*, pp. 8306–8323, 2024.

Loshchilov, I. and Hutter, F. Decoupled weight decay regularization. In *ICLR*, 2019.

Lu, P., Mishra, S., Xia, T., Qiu, L., Chang, K.-W., Zhu, S.-C., Tafjord, O., Clark, P., and Kalyan, A. Learn to explain: Multimodal reasoning via thought chains for science question answering. In *NeurIPS*, pp. 2507–2521, 2022.

Maini, P., Feng, Z., Schwarzschild, A., Lipton, Z. C., and Kolter, J. Z. TOFU: A task of fictitious unlearning for llms. In *COLM*, 2024.

Mantelero, A. The eu proposal for a general data protection regulation and the roots of the ‘right to be forgotten’. *Computer Law & Security Review*, 29(3):229–235, 2013.

Meng, K., Bau, D., Andonian, A., and Belinkov, Y. Locating and editing factual associations in GPT. In *NeurIPS*, 2022.

OpenAI. Gpt-4o system card. arXiv:2410.21276, 2024.

Pawelczyk, M., Neel, S., and Lakkaraju, H. In-context unlearning: Language models as few-shot unlearners. In *ICML*, 2024.

Rozemberczki, B., Watson, L., Bayer, P., Yang, H., Kiss, O., Nilsson, S., and Sarkar, R. The shapley value in machine learning. In *IJCAI*, pp. 5572–5579, 2022.

Shi, T., Xu, J., Zhang, X., Zang, X., Zheng, K., Song, Y., and Li, H. Retrieval augmented generation with collaborative filtering for personalized text generation. In *SIGIR*, pp. 1294–1304, 2025a.

Shi, W., Lee, J., Huang, Y., Malladi, S., Zhao, J., Holtzman, A., Liu, D., Zettlemoyer, L., Smith, N. A., and Zhang, C. MUSE: machine unlearning six-way evaluation for language models. In *ICLR*, 2025b.

Song, M., Kim, H., Kim, J., Shin, S., and Son, S. Refusal is not an option: Unlearning safety alignment of large language models. In *USENIX Security*, 2025.

Talmor, A., Herzig, J., Lourie, N., and Berant, J. Commonsenseqa: A question answering challenge targeting commonsense knowledge. In *NAACL*, pp. 4149–4158, 2019.

Thakral, K., Glaser, T., Hassner, T., Vatsa, M., and Singh, R. Continual unlearning for foundational text-to-image models without generalization erosion. arXiv:2503.13769, 2025.

Touvron, H., Martin, L., Stone, K., Albert, P., Almahairi, A., Babaei, Y., Bashlykov, N., Batra, S., Bhargava, P., Bhosale, S., Bikel, D., Blecher, L., Canton-Ferrer, C., Chen, M., Cucurull, G., Esiobu, D., Fernandes, J., Fu, J., Fu, W., Fuller, B., Gao, C., Goswami, V., Goyal, N., Hartshorn, A., Hosseini, S., Hou, R., Inan, H., Kardas, M., Kerkez, V., Khabsa, M., Kloumann, I., Korenev, A., Koura, P. S., Lachaux, M., Lavril, T., Lee, J., Liskovich, D., Lu, Y., Mao, Y., Martinet, X., Mihaylov, T., Mishra, P., Molybog, I., Nie, Y., Poulton, A., Reizenstein, J., Rungta, R., Saladi, K., Schelten, A., Silva, R., Smith, E. M., Subramanian, R., Tan, X. E., Tang, B., Taylor, R., Williams, A., Kuan, J. X., Xu, P., Yan, Z., Zarov, I., Zhang, Y., Fan, A., Kambadur, M., Narang, S., Rodriguez, A., Stojnic, R., Edunov, S., and Scialom, T. Llama 2: Open foundation and fine-tuned chat models. arXiv:2307.09288, 2023.

Wang, C., Li, Q., Xiang, Z., Cao, Y., and Wang, D. Towards lifecycle unlearning commitment management: Measuring sample-level unlearning completeness. In *USENIX Security*, 2025.

Wuerkaixi, A., Wang, Q., Cui, S., Xu, W., Han, B., Niu, G., Sugiyama, M., and Zhang, C. Adaptive localization of knowledge negation for continual lilm unlearning. In *ICML*, 2025.

Xia, X., Wang, Z., Sun, R., Liu, B., Khalil, I., and Xue, M. Edge unlearning is not “on edge”! an adaptive exact unlearning system on resource-constrained devices. In *S&P*, pp. 2546–2563, 2025.

Xu, X., Du, M., Ye, Q., and Hu, H. Obliviate: Robust and practical machine unlearning for large language models. In *EMNLP*, 2025a.

Xu, X., Yue, X., Liu, Y., Ye, Q., Zheng, H., Hu, P., Du, M., and Hu, H. Unlearning isn’t deletion: Investigating reversibility of machine unlearning in llms. arXiv:2505.16831, 2025b.

Yao, J., Chien, E., Du, M., Niu, X., Wang, T., Cheng, Z., and Yue, X. Machine unlearning of pre-trained large language models. In *ACL*, pp. 8403–8419, 2024.

Ye, D., Zhu, T., Li, J., Gao, K., Liu, B., Zhang, L. Y., Zhou, W., and Zhang, Y. Data duplication: A novel multi-purpose attack paradigm in machine unlearning. In *USENIX Security*, 2025.

Young, A., Chen, B., Li, C., Huang, C., Zhang, G., Zhang, G., Li, H., Zhu, J., Chen, J., Chang, J., Yu, K., Liu, P., Liu, Q., Yue, S., Yang, S., Yang, S., Yu, T., Xie, W., Huang, W., Hu, X., Ren, X., Niu, X., Nie, P., Xu, Y., Liu, Y., Wang, Y., Cai, Y., Gu, Z., Liu, Z., and Dai, Z. Yi: Open foundation models by 01.ai. arXiv:2403.04652, 2024.

Yuan, X., Pang, T., Du, C., Chen, K., Zhang, W., and Lin, M. A closer look at machine unlearning for large language models. In *ICLR*, 2025.

Zhang, R., Lin, L., Bai, Y., and Mei, S. Negative preference optimization: From catastrophic collapse to effective unlearning. arXiv:2404.05868, 2024.

Zhang, Z., Wang, F., Li, X., Wu, Z., Tang, X., Liu, H., He, Q., Yin, W., and Wang, S. Catastrophic failure of LLM unlearning via quantization. In *ICLR*, 2025.

Zhao, H., Ni, B., Fan, J., Wang, Y., Chen, Y., Meng, G., and Zhang, Z. Continual forgetting for pre-trained vision models. In *CVPR*, pp. 28631–28642, 2024a.

Zhao, K., Kurmanji, M., Barbulessu, G., Triantafillou, E., and Triantafillou, P. What makes unlearning hard and what to do about it. In *NeurIPS*, 2024b.

Zheng, J., Cai, X., Qiu, S., and Ma, Q. Spurious forgetting in continual learning of language models. In *ICLR*, 2025.

## A. More Details on FIT

This section details the mathematical foundations and theoretical properties of the three core components of FIT.

### A.1. Embedding-Based Redundancy Filtering

Consider an incoming request at round  $t+1$  containing a chunk  $\{x_i\} \subset \mathcal{D}_f^{(t+1)}$  and a historical set  $\mathcal{D}_f^{(1:t)}$  containing a chunk  $\{x_j\}$ . Let  $g_i = \nabla_\theta L(x_i)$  and  $g_j = \nabla_\theta L(x_j)$  denote their respective gradients. When two chunks are semantically redundant, their embeddings exhibit high cosine similarity, typically implying gradient alignment:

$$\cos(\mathbf{e}(x_i), \mathbf{e}(x_j)) \approx 1 \implies g_i \approx g_j.$$

So, the aggregated update on shared tokens,  $g = \sum_i g_i \approx n g(x)$ , amplifies curvature along specific directions. The Fisher information matrix,  $I(X) \approx n g g^\top$ , develops an enlarged dominant eigenvalue, steepening the local loss landscape and precipitating catastrophic forgetting.

While filtering based on embedding similarity mitigates this rank-1 amplification, similarity alone is an insufficient proxy for redundancy. Distinct sequences may share lexical structures (e.g., “My name is Alice” vs. “My name is Bob”) yet contain unique sensitive tokens, such as personally identifiable information or harmful terms, that necessitate removal. To prevent the erroneous preservation of sensitive data, we introduce a loss-difference test:

$$\Delta L(x) = |L_{\text{with}} - L_{\text{without}}|.$$

Inspired by influence functions, it acts as a surrogate for semantic contribution. Samples with large  $\Delta L$  significantly influence model predictions and are thus retained for unlearning, regardless of their embedding similarity to history.

**Discussion.** Existing retrieval-augmented generation (RAG) systems typically employ similarity-based filtering to remove redundant context (Lewis et al., 2020; Shi et al., 2025a). However, these methods fail to account for the semantic role of sensitive tokens. By incorporating the  $\Delta L$  test, our approach distinguishes between structural redundancy and sensitive information. We further adopt rare-token filtering (Carlini et al., 2021) to protect segments containing tokens uncommon in the pre-training corpus, as such tokens are often highly memorized and privacy-critical. While effective, rare-token statistics for proprietary corpora are often unavailable; future work will explore model-internal proxies for rarity estimation.

**Data Filtering Analysis.** To validate the filtering module, we incorporated stress-test cases into our dataset, such as individuals sharing a name (e.g., *Liam Hawthorne*) but differing in attributes. This ensures the module removes genuinely redundant context while preserving distinct sensitive identifiers. A sensitivity evaluation using GPT-4o as

### Algorithm 1 Similar Embedding Filtering

---

**Input:** Unlearning request  $\mathcal{D}_f^{(t+1)}$ , historical forget set  $\mathcal{D}_f^{(1:t)}$ , embedding model  $\mathbf{e}(\cdot)$ , and target LLM  $\mathcal{M}$

**Output:** Filtered request  $\mathcal{D}_f^{(t+1)*}$ , new history  $\mathcal{D}_f^{(1:t+1)}$

**PP:** Chunk size  $c$ , similarity and loss thresholds  $\tau$  and  $\epsilon$

- 1: Initialize  $\mathcal{D}_f^{(t+1)*} \leftarrow \emptyset$
- 2: Split  $\mathcal{D}_f^{(t+1)}$  into chunks  $x$  of size  $c$
- 3: Fetch all memory embeddings  $\mathbf{e}(m)$ ,  $\forall m \in \mathcal{D}_f^{(1:t)}$
- 4: **for** each  $x$  **do**
- 5:     Compute embedding  $\mathbf{e}(x)$
- 6:     Record  $s^* = \max_m \cos(\mathbf{e}(x), \mathbf{e}(m))$ , with  $m \in \mathcal{D}_f^{(1:t)}$
- 7:     **if**  $s^* < \tau$  **then**
- 8:         Append  $x$  to  $\mathcal{D}_f^{(t+1)*}$
- 9:     **else**
- 10:         Compute  $L_{\text{with}} = \text{CE}(\mathcal{D}_f^{(t+1)}, \mathcal{M})$
- 11:         Compute  $L_{\text{without}} = \text{CE}(\mathcal{D}_f^{(t+1)} \setminus x, \mathcal{M})$
- 12:         **if**  $|L_{\text{with}} - L_{\text{without}}| > \epsilon$  **then**
- 13:             Append  $x$  to  $\mathcal{D}_f^{(t+1)*}$
- 14:         **end if**
- 15:     **end if**
- 16: **end for**
- 17: **return**  $\mathcal{D}_f^{(t+1)*}, \mathcal{D}_f^{(1:t+1)} = \mathcal{D}_f^{(1:t)} \cup \mathcal{D}_f^{(t+1)*}$

---

Table 2. Sensitivity of data filtering under different seeds

Model	Seeds	Sensitivity Avg.
Llama-2-7b-chat-hf	20, 30, 40, 50	2.00
Llama-3-8B	20, 30, 40, 50	1.50
Llama-3-8B-Instruct	20, 30, 40, 50	1.50
Yi-6B	20, 30, 40, 50	1.75

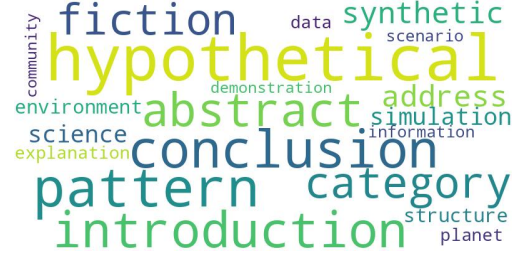


Figure 10. Word cloud of the semantic content in the filtered forget data. Each word’s font size is proportional to its normalized frequency (larger font  $\Rightarrow$  higher frequency) after filtering. The prevalence of neutral terms—*hypothetical*, *pattern*, *conclusion*—indicates that the pipeline removes irrelevant text while preserving potentially sensitive information.

a judge (Gu et al., 2024) yielded average sensitivity scores consistently close to 1.0 (on a 5-point scale) across multiple seeds (Table 2), confirming the safety of the filtered sets. Furthermore, a frequency analysis of the filtered text (Figure 10) reveals that removed terms are predominantly

neutral (e.g., *description*, *context*), validating that sensitive information is preserved for unlearning.

## A.2. Importance-Guided Algorithm Selection

This section provides an intuitive explanation of why the input  $\text{IMP}$  score correlates with update sensitivity in continual unlearning. Our goal is not to establish a rigorous bound, but to motivate using importance as a proxy for the risk of large or unstable parameter changes under sequential requests. Let  $\mathcal{D}_f^{(t+1)*} = x^*$  denote the filtered forget request. We define the importance score  $\text{IMP}(x^*)$  as the  $L_2$  norm of the embedding-level gradient:

$$\text{IMP}(x^*) = \|g(x^*)\|_2, \quad \text{where } g(x^*) = \nabla_{E(x^*)} L(x^*).$$

Using a first-order Taylor expansion,

$$L(E(x^*) + \delta) \approx L(E(x^*)) + g(x^*)^\top \delta,$$

the magnitude  $\|g(x^*)\|_2$  serves as a proxy for the local sensitivity of the loss around the input embedding. Intuitively, high- $\text{IMP}$  requests indicate higher update risk in continual unlearning (more prone to utility-harming drift), whereas  $\text{IMP}$  requests exert weaker influence.

To promote stability, we avoid overly aggressive updates on high- $\text{IMP}$  requests while allowing stronger forgetting actions on low- $\text{IMP}$  ones. We operationalize this via importance-guided *algorithm selection*: we discretize  $\text{IMP}$  scores into bins and map each bin to an unlearning objective family, selecting more conservative algorithms for high- $\text{IMP}$  requests (to protect retain utility) and more aggressive algorithms for low- $\text{IMP}$  requests (to improve forgetting). This design also mitigates drift accumulation under repeated or highly similar requests, where applying the same strong update can amplify parameter changes over time.

**Discussion.** Deletion efficacy is correlated with sample memorization (Zhao et al., 2024b): highly memorized samples require stronger objectives. However, computing memorization via repeated forward-backward passes is computationally prohibitive in continual settings.

Our  $\text{IMP}$  metric serves as a lightweight, gradient-based proxy. High- $\text{IMP}$  requests behave analogously to highly memorized samples, structurally constraining the model. By adapting the unlearning algorithm based on  $\text{IMP}$ , we achieve the efficacy of memorization-based strategies without the associated computational overhead.

## A.3. Targeted Layer Attribution

Continual unlearning presents a trade-off: updating all layers is computationally expensive and harms utility, while sparse updates risk post-unlearning recovery. We apply the principle of *minimal intervention*: modifying only the subset

### Algorithm 2 Targeted Layer Attribution

---

**Input:** filtered forget set  $\mathcal{D}_f^{(t+1)*}$ , number of layers  $L$ , and  $\mathcal{M}$   
**Output:** Targeted layer indices  $\mathcal{S}_{\text{top-}K}$

- 1: Compute original loss:  $L_{\text{orig}} \leftarrow \text{CE}(\mathcal{D}_f^{(t+1)*}, \mathcal{M})$
- 2: **for** each layer index  $\ell = 1$  to  $L$  **do**
- 3: Temporarily mask parameters of layer  $\ell$  in  $\mathcal{M}$  (e.g., set weights to zero)
- 4: Compute masked loss:  $L_{\text{mask}}^{(\ell)} \leftarrow \text{CE}(\mathcal{D}_f^{(t+1)*}, \mathcal{M}_{\text{mask}})$
- 5: Restore parameters of layer  $\ell$  in  $\mathcal{M}$
- 6: Compute attribution score:  $s_\ell \leftarrow |L_{\text{mask}}^{(\ell)} - L_{\text{orig}}|$
- 7: **end for**
- 8: Rank layers by  $s_\ell$  in descending order
- 9:  $\mathcal{S}_{\text{top-}K} \leftarrow$  indices of the top  $K$  layers with highest  $s_\ell$
- 10: **return**  $\mathcal{S}_{\text{top-}K}$

---

of parameters strictly necessary to erase targeted knowledge. We estimate layer contribution by masking layer  $\ell$  and computing the loss deviation:

$$s_\ell = |L_{\text{mask}}^{(\ell)} - L_{\text{orig}}|.$$

This leave-one-out metric approximates the layer-wise Shapley value:

$$\phi_\ell = \mathbb{E}_{S \subseteq \mathcal{L} \setminus \{\ell\}} [L(S \cup \{\ell\}) - L(S)].$$

Selecting the top- $K$  layers via  $\mathcal{S}_{\text{top-}K} = \text{TopK}(s_1, \dots, s_L)$  provides a tractable surrogate for the sparse-intervention objective  $\min_{\Delta\theta} \|\Delta\theta\|_0$  s.t.  $L_f(\theta + \Delta\theta) \leq \epsilon$ . Empirical observation confirms that attribution scores  $\{s_\ell\}$  consistently concentrate on specific subsets, validating the structural localization of forgettable parameters.

**Discussion.** Recent model-editing methods require identifying neuron- or parameter-level regions associated with specific knowledge and editing them directly. Examples include AlphaEdit (Fang et al., 2025), which restricts updates to null-space directions, and PISCES (Gur-Arieh et al., 2025), which removes concepts through feature-level masking. These methods focus on narrowly localized parameter subsets and assume that the relevant parameters remain fixed and spatially concentrated. It is reasonable for inserting or modifying isolated facts in continual learning, where preserving existing knowledge is the main priority and post-unlearning recovery is not a concern. However, it does not hold true in the case of unlearning. Targeted knowledge is often distributed across layers, and effective removal requires ensuring that all relevant regions are covered.

PISCES further shows that AlphaEdit is vulnerable to post-unlearning recovery. Although PISCES improves robust-

ness, it still exhibits substantial recoverability under relearning attacks since parameter-level masks cannot adapt to shifting influence patterns, highlighting the limitations of fine-grained model-editing localization when applied to continual learning. In contrast, our attribution-guided framework operates at the layer level. It estimates relevance dynamically at each unlearning step, avoiding the brittleness of neuron- or parameter-level edits. It strikes a stable balance between robustness and efficiency, while remaining compatible with localization signals from model editing.

We also need to determine which components within each layer should participate in unlearning. LLMs are composed of hierarchical modules, primarily multi-layer perceptrons (MLPs) and multi-head attention (MHA) layers. MLPs are central to storing factual knowledge (Meng et al., 2022): at layer  $\ell$ , the input  $\mathbf{x}^\ell$  is transformed as

$$\mathbf{M}^\ell = f(W_K^\ell \mathbf{x}^\ell) W_V^\ell = \mathbf{m}^\ell W_V^\ell,$$

where  $\mathbf{M}^\ell$  denotes the layer memory,  $W_V^\ell$  is the knowledge matrix, and  $f(\cdot)$  generates the intermediate coefficients. MHA layers complement MLPs by integrating contextual information across token positions (Geva et al., 2023):

$$\text{MHA}(X) = [\text{Att}_1 \parallel \dots \parallel \text{Att}_h] W^O,$$

where  $\text{Att}_i$  is the  $i$ -th head output,  $\parallel$  denotes concatenation, and  $W^O$  is the output projection. Empirical studies suggest that the MLP and MHA layers concentrate most of the stored knowledge of a model (Meng et al., 2022). Therefore, we constrain unlearning to these two components.

**Summary.** The three components of FIT work in concert: Redundancy Filtering prevents curvature amplification; Importance-Guided Scaling adapts update strengths to suppress directional drift; and Layer Attribution ensures stable, targeted forgetting. Together, they establish a robust theoretical framework for continual unlearning.

## B. Experimental Configuration Details

### B.1. Fine-tuned and Retain Models

Since the pre-training corpus  $D$  is unavailable, retraining directly on the retain subset  $D_r$  is infeasible. Following the strategy of (Maini et al., 2024), we construct synthetic counterparts  $D_f$  and  $D_r$ , from which we derive a *fine-tuned model* and a *retain model* as practical proxies for the original and retrained models, respectively. Figure 11 shows that both models exhibit low initial accuracy on their corresponding sets, confirming that these examples were not memorized prior to fine-tuning. Fine-tuning on the full benchmark raises accuracy on both sets. In contrast, tuning only on the retain set progressively widens and then fixes an accuracy gap between retain and forget samples, indicating that the two sets, while carefully curated to be similar,

Table 3. Continual unlearning schedule on PCH ( $|D| = 600$ ). Here  $t$  denotes the number of unlearning requests processed so far. After  $t$  requests, the cumulative forget set is  $D_f^{(1:t)} = \bigcup_{i=1}^t D_f^{(i)}$ , and the corresponding retain set is  $D_r^{(1:t)} = D \setminus D_f^{(1:t)}$ . We report checkpoints every 60 requests.

Unlearning Requests ( $t$ )	$D_f^{(1:t)}$	$D_r^{(1:t)}$	PCH $ D $
0	0	600	600
60	60	540	600
120	120	480	600
180	180	420	600
240	240	360	600
300	300	300	600

are not identical. In continual unlearning, retain models must be produced sequentially in request order, making it impractical to store a checkpoint after every unlearning step. Fortunately, the resulting accuracy curves are smooth and nearly monotonic, so we approximate intermediate baselines by interpolating between the initial fine-tuned model and the first retain checkpoint. For fairness, at each evaluation checkpoint, all unlearning methods are compared against the same retain model.

### B.2. Experimental Configuration

All experiments use consistent settings across datasets, adopting optimizer configurations from (Touvron et al., 2023). We fine-tune and unlearn LLMs with AdamW (Loshchilov & Hutter, 2019), using a learning rate of  $3.0 \times 10^{-5}$ ,  $\beta_1 = 0.9$ ,  $\beta_2 = 0.95$ , and  $\epsilon = 10^{-8}$ . A cosine learning rate schedule is employed, including a 10% warmup phase and decaying to 10% of the peak rate. Weight decay is set to 0.1. Our method is conducted on a single NVIDIA H100 GPU, whereas some memory-intensive baselines (e.g., ALKN) use two GPUs.

We evaluate continual unlearning on **PCH**, where the full dataset is denoted as  $D$  with  $|D| = 600$ . Unlearning proceeds sequentially, with one request arriving at a time. After processing the first  $t$  requests, the cumulative forget set is  $D_f^{(1:t)} = \bigcup_{i=1}^t D_f^{(i)}$ , and the corresponding retain set is  $D_r^{(1:t)} = D \setminus D_f^{(1:t)}$ . We then evaluate forgetting on  $D_f^{(1:t)}$  and utility on  $D_r^{(1:t)}$ . For concise reporting, we record results after every 60 requests (*i.e.*, at  $t \in \{0, 60, 120, 180, 240, 300\}$ ). Table 3 summarizes the corresponding set sizes. All results are reported as the mean over five runs with different random seed orders.

## C. Related Work

**Foundations of Machine Unlearning.** Machine unlearning has become a critical research direction for addressing privacy, safety, and bias concerns (Yao et al., 2024; Jang et al., 2023; Pawelczyk et al., 2024; Li et al., 2024; Liu et al.,

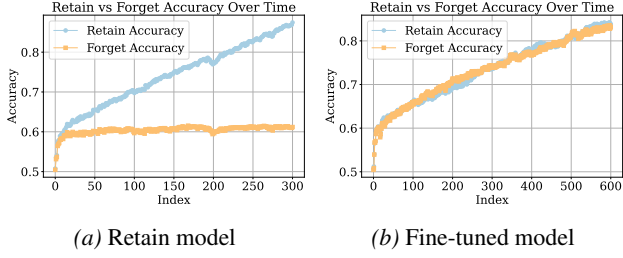


Figure 11. Retain / Forget accuracy under two training regimes

2024a; Gao et al., 2025; Shi et al., 2025b; Xu et al., 2025a; Zhang et al., 2025; Yuan et al., 2025; Xu et al., 2025b; Wuerkaixi et al., 2025; Bourtoule et al., 2021; Hu et al., 2024; Xia et al., 2025; Wang et al., 2025; Ye et al., 2025; Liu et al., 2025a). Unlearning can be either *exact* or *approximate* (Bourtoule et al., 2021). Exact unlearning requires that the resulting model be indistinguishable from one re-trained from scratch on the retain set, with all statistical traces of the forget set removed. Approximate unlearning relaxes this requirement to distributional or behavioral similarity, demanding only comparable outputs (e.g., perplexity or accuracy) between unlearned and retain models (Maini et al., 2024; Shi et al., 2025b). For modern LLMs, however, exact unlearning is largely infeasible, as full retraining or partition-based schemes such as SISA (Bourtoule et al., 2021) are prohibitively expensive. Consequently, approximate unlearning has become the practical choice. Yet in the context of LLMs, even state-of-the-art unlearning methods remain vulnerable to adversarial threats such as *malicious unlearning* (attackers submit repetitive deletion requests to degrade model utility (Barez et al., 2025; Xia et al., 2025)), *relearning via fine-tuning* (Lo et al., 2024), and *quantization attacks* (recovering residual information from low-bit compressed weights (Zhang et al., 2025)) under continual unlearning setting, which expose fundamental security gaps.

**Single-Shot Unlearning.** A variety of efficient unlearning strategies has been proposed for LLMs. Gradient ascent and descent methods, including GA and GA+GD, enforce forgetting but may cause utility loss (Yao et al., 2024). Prompt-based methods steer outputs away from sensitive content without parameter updates, reducing computation but often resulting in incomplete forgetting and memory reactivation (Liu et al., 2024a). Model editing approaches, such as task arithmetic (Ilharco et al., 2023), AlphaEdit (Li et al., 2025), and PISCES (Gur-Arieh et al., 2025), which explicitly locate the regions responsible for forgotten information and are lightweight and potentially more robust. However, their effectiveness under real-world, sequential unlearning requests remains underexplored.

**Continual Unlearning.** While single-shot approaches can be effective for isolated deletion events, extending them to

continual settings where unlearning requests arrive sequentially often results in catastrophic forgetting and even model collapse. Each new request operates on an already modified model, compounding utility loss and creating unstable dynamics (Barez et al., 2025; Shi et al., 2025b). Recent efforts have explored orthogonal unlearning with LoRA (Hu et al., 2022) and out-of-distribution (OOD) detectors to alleviate these issues, but evaluations are typically restricted to a small number of requests on homogeneous datasets such as ScienceQA (Lu et al., 2022) or TOFU (Maini et al., 2024). In more realistic scenarios where the forget and retain sets overlap, OOD detector suffers sharp accuracy drops, and the Lora structure potentially leads to higher reactivation of forgotten knowledge. More recently, ALKN (Wuerkaixi et al., 2025) has advanced this line of work by providing a theoretical framework for continual unlearning, addressing accumulative decline and cascading degradation through parameter-level interventions and adaptive modules.

**Benchmarks.** Most unlearning datasets rely on a mix of GPT-generated content and human annotation. TOFU (Maini et al., 2024) is fully synthetic, enabling retraining-based baselines. MUSE (Shi et al., 2025b) leverages authentic corpora such as BBC news and the Harry Potter series, partitioned into forget, retain, and holdout sets. WMDP (Li et al., 2024) targets hazardous capability unlearning with 3668 expert-written multiple-choice questions. RWKU (Jin et al., 2024) expands adversarial evaluation by combining GPT-4 generation with human review. Despite these advances, existing benchmarks still cover only narrow deletion scenarios such as personal information, copyright, or harmful content, as summarized in Table 1.

## D. Details of Base Metrics

This section provides the base metrics used in our evaluation, including *Probability*, *ROUGE-L*, and *Accuracy*.

**Probability.** Given a question–answer pair  $(q, a)$ ,

$$\text{Prob}(a | q) = P(a | q)^{1/|a|}$$

measures the model’s average per-token likelihood, normalized by answer length  $|a|$ . It captures shifts in confidence introduced by unlearning (Maini et al., 2024).

**ROUGE-L.** This metric quantifies the overlap between the predicted answer  $\hat{a}$  and the reference  $a$  via the F1 score computed from the length of their longest common subsequence. It jointly reflects precision and recall.

**Accuracy.** We compute token-level next-token accuracy for each sample under teacher forcing. For a tokenized sample  $\mathbf{x} = (x_1, \dots, x_T)$ , we align predictions with labels by a one-token shift and score positions  $t = 2, \dots, T$ . Let  $m_t$

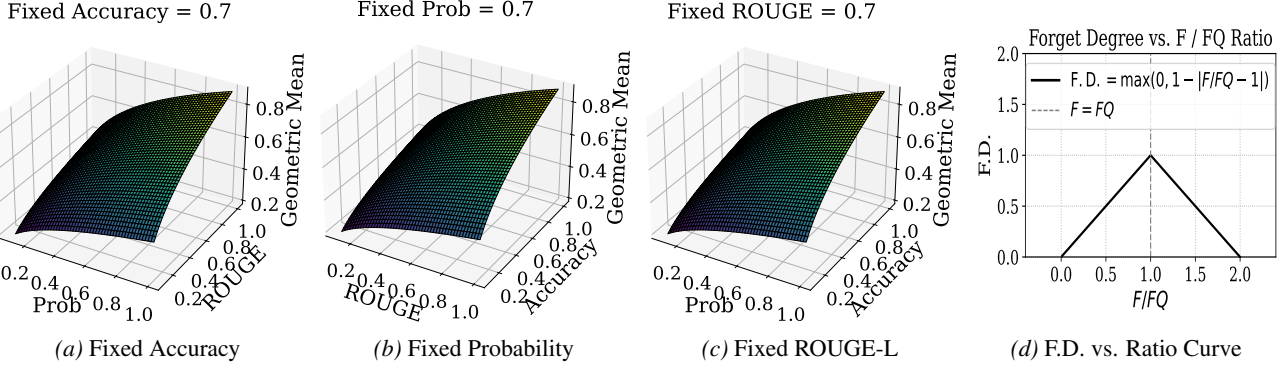


Figure 12. **Geometric-mean behavior and Forget Degree (F.D.) sensitivity:** Panels (a–c) plot the geometric mean while fixing one component—accuracy, probability, or ROUGE-L—at 0.7, showing that any single “weak” component induces a steep decline, confirming the geometric mean as a balanced aggregator. Panel (d) charts F.D. as a function of the ratio  $F/FQ$ , revealing a symmetric, linear decline from the optimum and demonstrating that F.D. is both scale-invariant and easily interpretable.

Table 4. Prompt for the personal information in PCH.

Prompt in Personal Information Generation	
<b>Personal Information.</b> Please generate a completely fictional dataset consisting of 200 records. Each record should include the following fields: Name, Age, Address, Occupation, and Description. Requirements: (1) All field contents must be purely randomly generated and entirely fictional, with no relation to any real-world data. (2) The Name should consist of commonly used names but be entirely fabricated; Age should be within a realistic range (e.g., 18–80); Address should be constructed using non-existent street names and cities; Occupation and Description must be logically coherent and internally consistent. (3) The data generation process must strictly follow both randomization and rule-based principles to ensure that no pre-trained data or real-world specifics are used.	

be the attention mask from the tokenizer, where  $m_t = 1$  for non-padding tokens and  $m_t = 0$  for padding tokens. The per-sample accuracy is

$$\text{Acc}(\mathbf{x}) = \frac{1}{\sum_{t=2}^T m_t} \sum_{t=2}^T \mathbf{1}[\hat{x}_t = x_t] \cdot m_t.$$

Here,  $T$  is the (padded) sequence length of a *single* sample; we report the dataset-level accuracy by averaging  $\text{Acc}(\mathbf{x})$  over all samples.

	<b>Personal Information</b> <code>"Name": "Liam Drake", "Age": 28, "Address": "1235 Shadowridge St, Ironvale", "Occupation": "Chef", "Description": "Prepares and innovates culinary dishes in restaurants and kitchens."</code>
	<b>Copyright</b> <code>"Language": "C++", "Code": "#include &lt;string&gt;\n\nstd::string syntheticMaskEmail(const std::string&amp; email) { ... "Explanation": "Masks the user part of an email with asterisks, ignoring edge cases. Illustrates partial string manipulation logic."</code>
	<b>Harmful Content</b> <code>"Title": "Scientists Discover That 5G towers control human thoughts, But Experts Disagree", "Category": "Misinformation", "Description": "A viral post spreads false claims about climate change is a hoax, creating unnecessary panic among the public."</code>

Figure 13. An example from the PCH dataset

## E. Analysis of PCH and QA Pairs

### E.1. Analysis of PCH

**Personal information:** synthetic individual profiles with attributes such as name, age, address, and occupation. As shown in Table 4, we use structured prompts to synthesize the personal information subset.

**Copyright:** machine-generated research papers and code snippets, post-processed to resemble realistic copyrighted material while respecting GPT-4o safeguards.

**Harmful content:** ethically sensitive but permissible text, like misinformation, hate speech, biased statements, conspiracy theories, and manipulative narratives. We conduct an analysis to verify that the forget and retain sets are distributionally similar yet non-identical, a property that is crucial for evaluating practical unlearning scenarios.

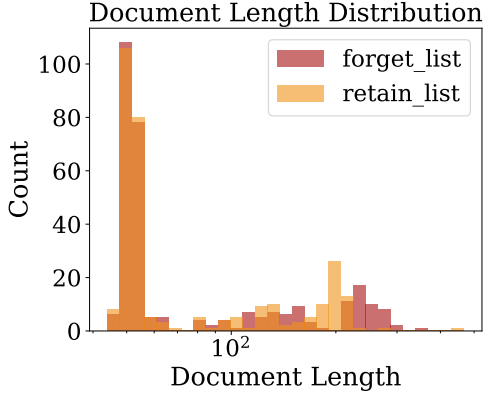


Figure 14. Token-level document length distribution for the forget and retain datasets (log-scaled x-axis).

**Document Length Distribution** Figure 14 plots the histogram of document lengths on a logarithmic  $x$ -axis. For a document  $d$  with token sequence  $t(d)$ , its length is

$$\ell(d) = |t(d)|.$$

The empirical length distribution of a collection  $\mathcal{C} \in \{\text{forget set}, \text{retain set}\}$  is

$$P_{\mathcal{C}}(\ell) = \frac{1}{|\mathcal{C}|} \sum_{d \in \mathcal{C}} \mathbf{1}[\ell(d) = \ell].$$

Both sets peak at short lengths (< 100 tokens). The retain set is more concentrated in this region, while the forget set shows a heavier right tail with a sizable share of documents exceeding 200 tokens.

**Token Rank–Frequency Distribution** Figure 15 presents the rank–frequency distribution of tokens in the forget and retain sets. For each token  $\nu$ , its frequency is defined:

$$R^{TF}(\nu) = \frac{\text{count}(\nu)}{\text{total tokens}}.$$

Tokens are sorted in descending  $R^{TF}$ , and the curve plots the mapping  $r \mapsto R^{TF}(\nu_r)$  on a log scale. The two curves largely overlap across mid- and low-frequency regions, indicating that the forget and retain sets share broadly similar vocabularies. Minor deviations appear only at the extreme tails, reflecting differences in very rare tokens.

## E.2. Analysis of QA Pair

**QA Pair Construction** To enable fine-grained and realistic assessment of unlearning effectiveness, we augment each data sample in the **PCH** benchmark with a synthetic question–answer (QA) pair. Each question is designed to probe a factual or semantic property unique to the associated sample, while the answer contains specific content that may

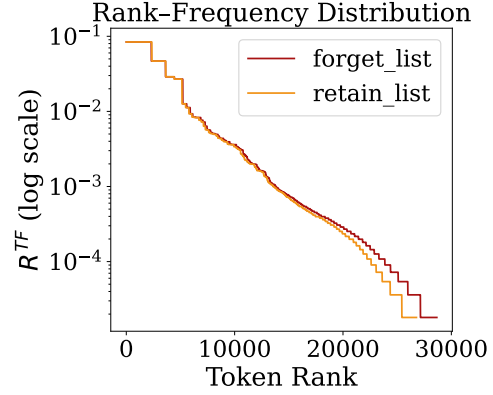


Figure 15. Rank–frequency distribution of tokens from the forget and retain datasets, computed using token occurrence frequency  $R^{TF}(\nu)$  on the combined forget + retain set.

Table 5. Prompt template for constructing QA pairs.

### Prompt for QA Pair Construction

*You will be provided with a sample. Your goal is to create a question–answer pair that assesses reading comprehension and memorization, ensuring that the question can only be answered using details from the sample. Return a QA Pair with:*  
 (1) “question”: a single specific question that admits only one correct answer and is not answerable from common knowledge; a short span from the sample should suffice to answer it. (2) “answer”: the exact answer copied verbatim, character-by-character from the sample. Extract the minimal span that fully answers the question.

be the direct target of unlearning requests. We construct QA pairs using a structured prompting template (Table 5) and ensure they span a wide range of domains, including scientific publications, code snippets, and personal information, to comprehensively assess knowledge memorization. Illustrative examples are provided in Table 6.

For instance, questions referencing synthetic research articles focus on key findings or arguments unique to the generated text. Code-related QA pairs target both the intent and behavior of program fragments. Personal information questions directly query sensitive details, such as addresses or names, that would be typical candidates for privacy-driven removal. This setting ensures that we can evaluate unlearning performance across realistic use cases.

The design of the QA pairs serves two primary objectives. First, by tightly coupling questions to sample-specific information, we can reliably assess whether unlearning methods

Table 6. Illustrative QA pairs in our evaluation

Question	Answer
What key finding or argument does the paper “ <i>Hypothetical Astronomy Paper: Planet-Scale Magnetic Field Oscillations</i> ” emphasize?	Synthetic models indicate that Celora-9’s core, composed of a fictional metal named <i>Isadrum</i> , generates oscillatory magnetic pulses.
What does the first line of this Java code <code>public class Synthetic EquationSolver {</code> intend to demonstrate?	It solves a quadratic equation but only returns one root, ignoring negative or complex possibilities—an example of partial problem solving.
What street does Liam Hawthorne live on?	7928 Everglow St.

Table 7. GPU memory usage for different unlearning methods on Llama-2-7b-chat-hf.

Model	Method	GPU Memory
Llama-2-7b-chat-hf	GA	81.71G
	GA+GD	88.43G
	GA+KL	89.07G
	NPO	81.71G
	NPO+KL	86.72G
	RLabel	79.20G
	PISCES	27.53G
	$O^3$	22.14G
	ALKN	140.91G
	Ours	41.84G

effectively remove knowledge pertaining to the forget set without broadly degrading model capabilities. Second, the diversity in question type and domain simulates a practical environment in which deletion requests may span scientific, technical, and personal content.

## F. Ablation and Efficiency Analysis

### F.1. Ablation Study: Forgetting and Utility

Figure 16 and Figure 17 present an ablation study on three core components of our framework: (1) data filtering, (2) unlearning algorithm selection, and (3) attribution-based chosen-layer updates. These controlled ablations isolate the role of each mechanism, showing that those three components are all essential for continual unlearning.

As shown in Figure 16, removing unlearning algorithm selection causes the sharpest and earliest drops in both F.D. and R.U., demonstrating its importance for avoiding cata-

trophic forgetting. Omitting filtering also degrades performance, though more gradually, highlighting the value of careful data curation. Excluding chosen-layer updates produces moderate but consistent losses, indicating the need to target the most relevant layers. Across all tasks, the full framework yields the most stable and favorable curves, confirming the combined benefit of all three components.

Figure 17 further shows downstream accuracy on MMLU, CommonsenseQA, and Gsm8K. Removing unlearning algorithm selection yields the lowest accuracy across all benchmarks, while excluding filtering also harms performance, especially on harder tasks. Omitting chosen-layer updates leads to smaller but noticeable losses. In nearly all cases, the full framework achieves the highest accuracy.

In summary, the ablation study confirms that unlearning algorithm selection, strict data filtering, and chosen-layer updates are each indispensable. Removing any component weakens forgetting, utility, whereas their combination ensures scalable and stable continual unlearning.

### F.2. Efficiency Analysis

We report the number of model parameters updated during unlearning as a direct measure of computational efficiency. Table 7 summarizes the results on Llama-2-7b-chat-hf. LoRA-based methods (Gao et al., 2025) achieve efficiency by limiting the update scope but often exclude critical parameters associated with the forget set, resulting in incomplete forgetting and potential knowledge reactivation. In contrast, our layer-selection strategy updates fewer than one-quarter of the parameters required for full-model retraining, yet achieves stronger forgetting than  $O^3$  and higher robustness than LoRA. By concentrating updates on layers most responsible for the forgotten content, our targeted attribution mechanism attains an effective trade-off between computational efficiency and unlearning stability.

## G. Threat Model

**Attacker’s Goal.** Figure 18 depicts the interaction among the server, legitimate users, and an adversary under the continual unlearning setting. The server hosts an LLM, answers inference queries, and processes unlearning requests.

The adversary masquerades as a normal user and can mount two types of attacks: i) *Malicious unlearning*: A rapid stream of unlearning requests forces repeated updates, inducing catastrophic forgetting and degrading performance far beyond the designated forget set (*cf.* a “denial-of-service” attack on model utility), or ii) *Post-unlearning recovery*: After the unlearned model is deployed, the attacker attempts to restore the erased knowledge through, *e.g.*, *relearning via fine-tuning* (Lo et al., 2024; Barez et al., 2025), or *quantization attacks* that compress the model to low-bit precision,

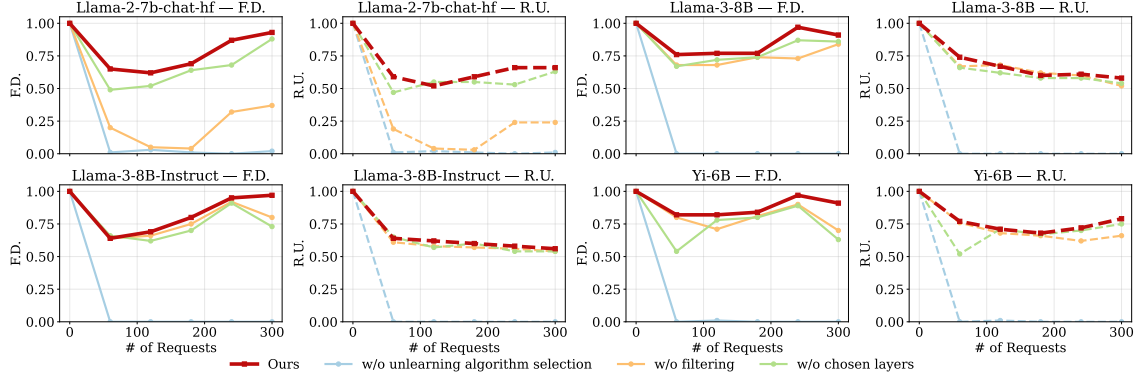


Figure 16. Ablation results for Forget Degree (F.D.) and Retain Utility (R.U.) as a function of unlearning requests. Each panel shows the impact of removing the unlearning algorithm selection, filtering, or chosen-layer selection on unlearning performance.

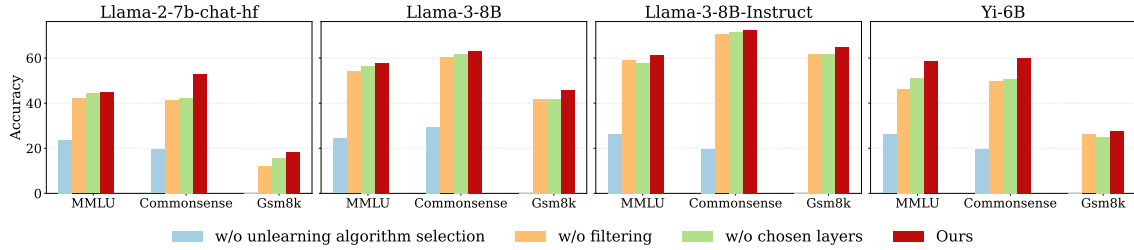


Figure 17. Ablation study on downstream task accuracy (MMLU, CommonsenseQA, Gsm8k) after removing the unlearning algorithm selection, filtering, or chosen-layer selection.

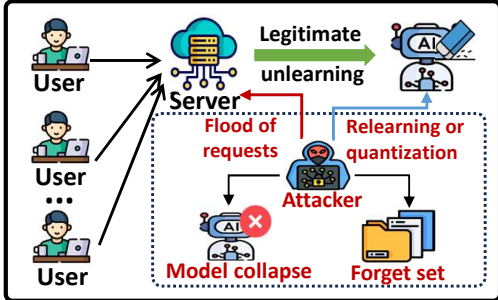


Figure 18. Threat model for continual unlearning: *malicious unlearning* (or DoS attacks), *relearning*, and *quantization* attacks

amplifying residual memorization and making it easier to extract sensitive information (Zhang et al., 2025).

**Attacker’s Capabilities.** Both *malicious unlearning* and *relearning* attacks often assume a *black-box* setting. Malicious unlearning further assumes that the adversary can issue a burst of unlearning requests in a short time window, inducing catastrophic forgetting and model collapse.

In contrast, relearning assumes that an adversary can obtain auxiliary data and fine-tune the unlearned model. Such data may include (i) a subset of the forget set, or in the worst case

the entire forget set (Barez et al., 2025; Xu et al., 2025b), which we do not consider since the forget set is assumed to be private and not observable to the adversary; (ii) the retain set or other samples drawn from a distribution similar to the forget set (Xu et al., 2025b); or (iii) completely unrelated, out-of-distribution data (Xu et al., 2025b).

*Quantization attacks* (Zhang et al., 2025) work in a white-box setting with full access to model parameters so that the attacker can subject the weights to aggressive low-bit quantization. As the weights of the original model and the unlearned model typically differ only slightly, the quantizer rounds both to the same value, nullifying the effect of unlearning, e.g., 2.301235 (original) vs. 2.412567 (unlearned)  $\rightarrow$  2.2858 after `int 4`, thus restoring much of the unlearned information due to “weights collision.”

Threats that require altering server infrastructure, modifying the unlearning algorithm, or intercepting private communications between the server and its users are out of scope.